Mid-infrared source with 0.2 J pulse energy based on nonlinear conversion of Q-switched pulses in $ZnGeP_2$

Magnus W. Haakestad,* Helge Fonnum, and Espen Lippert

Norwegian Defense Research Establishment (FFI), P. O. Box 25, NO-2027 Kjeller, Norway

*Magnus-W.Haakestad@ffi.no

Abstract: Mid-infrared (3–5 μm) pulses with high energy are produced using nonlinear conversion in a $ZnGeP_2$-based master oscillator-power amplifier, pumped by a Q-switched cryogenic Ho:YLF oscillator. The master oscillator is based on an optical parametric oscillator with a V-shaped 3-mirror ring resonator, and the power amplifier is based on optical parametric amplification in large-aperture $ZnGeP_2$ crystals. Pulses with up to 212 mJ energy at 1 Hz repetition rate are obtained, with FWHM duration 15 ns and beam quality $M^2 = 3$.

OCIS codes: (140.3070) Infrared and far-infrared lasers; (190.4410) Nonlinear optics, parametric processes; (190.4970) Parametric oscillators and amplifiers.

References and links

1. I. T. Sorokina and K. L. Vodopyanov, eds., *Solid-State Mid-Infrared Laser Sources*, *Topics in Applied Physics* (Springer, 2003), Vol. 89.
2. V. Petrov, "Parametric down-conversion devices: the coverage of the mid-infrared spectral range by solid-state laser sources," Opt. Mater. **34**, 536–554 (2012).
3. K. T. Zawilski, P. G. Schunemann, S. D. Setzler, and T. M. Pollak, "Large aperture single crystal $ZnGeP_2$ for high-energy applications," J. Cryst. Growth **310**, 1891–1896 (2008).
4. F. Ganikhanov, T. Caughey, and K. L. Vodopyanov, "Narrow-linewidth middle-infrared $ZnGeP_2$ optical parametric oscillator," J. Opt. Soc. Am. B **18**, 818–822 (2001).
5. M. W. Haakestad, G. Arisholm, E. Lippert, S. Nicolas, G. Rustad, and K. Stenersen, "High-pulse-energy mid-infrared laser source based on optical parametric amplification in $ZnGeP_2$," Opt. Express **16**, 14263–14273 (2008).
6. G. Stoeppler, N. Thilmann, V. Pasiskevicius, A. Zukauskas, C. Canalias, and M. Eichhorn, "Tunable mid-infrared $ZnGeP_2$ ristra opo pumped by periodically-poled Rb:KTP optical parametric master-oscillator power amplifier," Opt. Express **20**, 4509–4517 (2012).
7. P. A. Budni, C. R. Ibach, S. D. Setzler, L. A. Pomeranz, M. L. Lemons, P. A. Ketteridge, E. J. Gustafson, Y. E. Young, P. G. Schunemann, T. M. Pollak, R. T. Castro, and E. P. Chicklis, "20 mJ, 3-5 micron $ZnGeP_2$ optical parametric oscillator pumped by a 2.09 micron Ho:YAG laser," in "Advanced Solid-State Photonics," (Optical Society of America, 2003). Paper PD12.
8. A. Dergachev, D. Armstrong, A. Smith, T. Drake, and M. Dubois, "High-power, high-energy ZGP OPA pumped by a 2.05-μm Ho:YLF MOPA system," Proc. SPIE **6875**, 687507 (2008).
9. G. Stoeppler, M. Schellhorn, and M. Eichhorn, "Ho3+:LLF MOPA pumped RISTRA ZGP OPO at 3-5 μm," Proc. SPIE **8604**, 86040I (2013).
10. G. A. Rines, D. M. Rines, and P. F. Moulton, "Efficient, high-energy, KTP optical parametric oscillators pumped with 1 micron Nd-lasers," in "Advanced Solid State Lasers," (Optical Society of America, 1994), p. PO9.
11. H. Ishizuki and T. Taira, "Half-joule output optical parametric oscillation by using 10-mm-thick periodically poled Mg-doped congruent $LiNbO_3$," Opt. Express **20**, 20002–20010 (2012).
12. B. C. Johnson, V. J. Newell, J. B. Clark, and E. S. McPhee, "Narrow-bandwidth low-divergence optical parametric oscillator for nonlinear frequency-conversion applications," J. Opt. Soc. Am. B **12**, 2122–2127 (1995).
13. Y. Ehrlich, S. Pearl, and S. Fastig, "High brightness tunable tandem optical parametric oscillator at 8-12 μm," in "Advanced Solid-State Photonics," (Optical Society of America, 2004), p. TuB15.

#207849 - $15.00 USD Received 7 Mar 2014; accepted 25 Mar 2014; published 2 Apr 2014

14. D. J. Armstrong and A. V. Smith, "Demonstration of improved beam quality in an image-rotating optical parametric oscillator," Opt. Lett. **27**, 40–42 (2002).
15. A. Dergachev, D. Armstrong, A. Smith, T. Drake, and M. Dubois, "3.4-μm ZGP RISTRA nanosecond optical parametric oscillator pumped by a 2.05-μm Ho:YLF MOPA system," Opt. Express **15**, 14404–14413 (2007).
16. A. V. Smith and M. S. Bowers, "Image-rotating cavity designs for improved beam quality in nanosecond optical parametric oscillators," J. Opt. Soc. Am. B **18**, 706–713 (2001).
17. G. Rustad, "Investigation on how non-collinear phase matching can improve beam quality from optical parametric oscillators," in "50 years of nonlinear optics - NLO 50 international symposium," (Barcelona, Spain, 2012), Paper no. TP.GR.
18. W. R. Bosenberg and D. R. Guyer, "Broadly tunable, single-frequency optical parametric frequency-conversion system," J. Opt. Soc. Am. B **10**, 1716–1722 (1993).
19. G. Arisholm, Ø. Nordseth, and G. Rustad, "Optical parametric master oscillator and power amplifier for efficient conversion of high-energy pulses with high beam quality," Opt. Express **12**, 4189–4197 (2004).
20. P. Ruan, J. Xie, L. Zhang, J. Guo, J. Xie, G. Yang, D. Li, Q. Pan, G. Tan, F. Meng, and S. Li, "Computer modeling and experimental study of non-chain pulsed electric-discharge DF laser," Opt. Express **20**, 28912–28922 (2012).
21. A. Zajac, M. Skorczakowski, J. Swiderski, and P. Nyga, "Electrooptically Q-switched mid-infrared Er:YAG laser for medical applications," Opt. Express **12**, 5125–5130 (2004).
22. V. V. Badikov, P. F. Gonzalez-Diaz, M. Santos, C. Siguenza, G. S. Shevyrdyaeva, A. S. Solodukhin, and S. A. Trushin, "Wide-aperture $AgGaSe_2$ crystals for high-energy second-harmonic and sum-frequency generation of CO_2 laser radiation and their application," Proc. SPIE **2800**, 153–156 (1996).
23. Q. Liu, Z. Zhang, J. Liu, and M. Gong, "100 Hz high energy $KTiOAsO_4$ optical parametric oscillator," Infrared Phys. Techn. **61**, 287–289 (2013).
24. E. Lippert, H. Fonnum, G. Arisholm, and K. Stenersen, "A 22-watt mid-infrared optical parametric oscillator with V-shaped 3-mirror ring resonator," Opt. Express. **18**, 26475–26483 (2010).
25. G. Arisholm, "Quantum noise initiation and macroscopic fluctuations in optical parametric oscillators," J. Opt. Soc. Am. B **16**, 117–127 (1999).
26. H. Fonnum, E. Lippert, and M. W. Haakestad, "550 mJ Q-switched cryogenic Ho:YLF oscillator pumped with a 100 W Tm:fiber laser," Opt. Lett. **38**, 1884–1886 (2013).
27. G. Rustad, G. Arisholm, and Ø. Farsund, "Effect of idler absorption in pulsed optical parametric oscillators," Opt. Express **19**, 2815–2830 (2011).

1. Introduction

Laser sources emitting pulses with megawatt peak power and nanosecond duration in the mid-infrared wavelength range have a number of applications including spectroscopy, remote sensing, and surgery [1]. Nonlinear devices, such as optical parametric oscillators (OPOs) and amplifiers (OPAs), are particularly attractive because they can reach wavelengths where conventional laser lines are lacking. One promising material for such devices is zinc germanium phosphide (ZGP) due to its high nonlinear coefficient, reasonably high damage threshold, good transmission in the mid-infrared range, and high thermal conductivity [2, 3].

ZGP needs to be pumped at a wavelength > 2 μm to avoid absorption. One way to achive this is to use a two-stage system, where a Nd laser is used to pump a suitable nonlinear crystal, such as $KTiOPO_4$, and the output from the nonlinear interaction in the first stage is utilized to pump the ZGP stage [4–6]. An alternative, which avoids the first conversion stage, is to pump ZGP directly with a Ho-based laser near 2.1 μm [7–9].

The beam diameter must be large when generating nanosecond pulses with high pulse energy, to avoid exceeding the damage threshold of the nonlinear crystals. OPOs have been scaled to several hundred millijoules [10, 11], but obtaining good beam quality directly from an OPO with a large beam diameter is challenging due to the high Fresnel-number of the resonator, which results in a large number of transverse modes. This problem can be addressed using confocal unstable resonators [12, 13], or by image-rotating resonators [14, 15]. Image-rotation works best when there is considerable lateral walk-off between the signal and idler beams in the nonlinear crystal [16, 17]. For collinear nonlinear interaction, this is only the case for type II phase-matching, which is not possible for ZGP in the 3–5 μm range when pumping at 2.1 μm.

An alternative solution, which avoids the need for OPOs with large beam diameter, is the master oscillator-power amplifier (MOPA) approach. Here, a master OPO is pumped with a low

#207849 - $15.00 USD Received 7 Mar 2014; accepted 25 Mar 2014; published 2 Apr 2014

to moderate energy beam, and is optimized for providing output pulses with good beam quality. The signal and/or idler from the master OPO is then used as a seed in an optical parametric amplifier, which can provide output pulses with good beam quality, also for beams with large diameter [5, 8, 18, 19].

Several sources have previously been used to generate nanosecond pulses with megawatt peak power in the 3–5 μm wavelength range. Ruan et al. have obtained pulses with an energy of 4.95 J and 149 ns duration at $\sim$3.8 μm wavelength from a deuterium fluoride laser [20], but they do not report the beam quality. Zajac et al. demonstrated 137 mJ in 91 ns long pulses from a Q-switched Er:YAG laser at 2.94 μm [21], without stating the beam quality. Badikov et al. obtained up to 350 mJ in $\sim$100 ns pulses at 5.3 μm from a frequency-doubled multi-transverse-mode CO_2 laser [22]. Liu et al. obtained 34 mJ pulses at 3.5 μm, with a duration of 15 ns, from a $KTiOAsO_4$ OPO [23], but the beam quality was not reported. Dergachev et al. obtained 30 mJ at 3.4 μm from a ZGP MOPA with $\sim$20 ns pulse duration [8], with a beam quality of $M^2 \leq 1.8$ from the master oscillator, but the beam quality of the OPA was not stated. Haakestad et al. obtained 33 mJ at 3–5 μm from a ZGP MOPA, with pulse duration 6 ns, and a beam quality M^2=2–4 [5].

We here demonstrate a ZGP-based MOPA, with more than 200 mJ output energy in 15 ns pulses, with beam quality $M^2 = 3$, pumped at 2.05 μm by a cryogenically cooled Ho:YLF laser. The master OPO is based on a V-shaped 3-mirror ring resonator [24], and the power OPA is based on 1–3 large-aperture ZGP crystals. The design of the entire setup, including the pump laser, was aided by Sisyfos (Simulation System for Optical Science), an in-house simulation software for lasers and nonlinear interactions [25].

2. Experimental setup and simulations

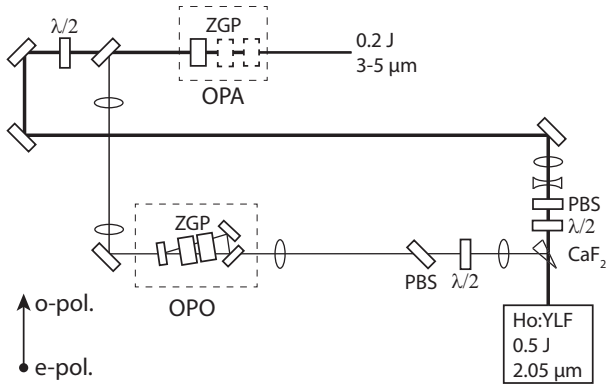

Fig. 1. Schematic overview of the ZGP-based MOPA. PBS: polarizer, $\lambda/2$: half-wave plate @ 2.05 μm, CaF_2: CaF_2 wedge. The number of ZGP crystals in the OPA were 1–3 in the experiments.

An overview of the experimental setup is given in Fig. 1. The Q-switched cryogenic Ho:YLF oscillator provides 0.5 J pulses at 2.05 μm wavelength and 1 Hz repetition rate [26], and has a FWe^{-2}M beam diameter of 6.1 mm. The beam quality of the pump laser is $M^2 = 1.5$, and the pulse duration (FWHM) is 16 ns. Although the pump laser can operate at higher repetition rates, with 0.3 J pulse energy at 20 Hz [26], we operated it at 1 Hz here to maximize the pulse energy. The pump beam for the OPO was obtained using one reflection from a CaF_2 wedge, while the transmitted pump was directed to the OPA. The maximum pump energy at the OPA was 381 mJ, while 35 mJ was reflected from each surface of the CaF_2 wedge. About 10% of the

#207849 - $15.00 USD Received 7 Mar 2014; accepted 25 Mar 2014; published 2 Apr 2014

available pump energy was lost in the optical components from the laser to the OPA crystals. Relay imaging telescopes were used to reduce the OPO pump beam diameter (FWe^{-2}M) to 2.7 mm and expand the output beam (signal and idler) from the OPO to a FWe^{-2}M diameter of 8.7 mm. The pump beam for the OPA was expanded to a FWe^{-2}M diameter of 8.6 mm with a Galilean telescope.

The ZGP crystals used in the OPO and OPA were manufactured by Inrad. They were cut at $\theta = 54^{\circ}$ for type I phase-matching and angle-tuned to provide a signal and idler wavelength of $\sim$3.7 μm and $\sim$4.6 μm, respectively. Crystals with 6 mm length and apertures of 10 mm $\times$ 12 mm and 12 mm $\times$ 14 mm were used in the experiment. Pump transmission (o-polarisation) through the AR coated crystals varied within the range 84–92%, while the transmission at 3–5 μm (e-polarisation) was 93–97%. For a given crystal aperture, the maximum pulse energy is limited by the maximum allowable peak fluence, which is determined by the damage threshold of the crystal. The damage threshold of the nonlinear crystals was investigated by reducing the pump beam diameter to 1 mm and visually inspect the crystal's entrance and exit surface during exposure of 250 pump pulses at constant energy. The peak fluence was gradually increased in steps of 0.1 J/cm^2, and visual damage occurred for a peak fluence of 2.3 J/cm^2. In the experiments, the total peak fluence of the OPO and OPA was kept below 0.8 J/cm^2 and 1.2 J/cm^2, respectively, to operate well below the estimated damage threshold of the nonlinear crystals. The safety margin for the peak fluence of the OPO was chosen especially large to ensure reliable long-term operation. During the experiments a $\sim$0.5 mm diameter damage occurred on the front surface of the first OPA crystal. No further damages were observed.

2.1. Master oscillator

The master OPO is based on a V-shaped 3-mirror ring resonator [24], which is schematically shown in Fig. 1. The main advantages of such a resonator is two-pass pumping without pump feedback into the laser, simple alignment, compactness, and reduced fluence because the forward and backward propagating beams are non-overlapping.

Numerical simulations using realistic pump and crystal parameters (including a linear pump transmission of 84% and a signal and idler transmission of 94% in the nonlinear crystal) were carried out to optimize the design of the OPO. A selection of the simulation results are shown in Fig. 2, where the performance of a singly resonant and a doubly resonant configuration are compared for different crystal lengths. The pump diameter (FWe^{-2}M) was 3.0 mm, the out-coupling 0.5, the pump energy 25 mJ, and the pump duration (FWHM) 15 ns in the simulations. The fluctuations in the simulation results are due to (i) that a pump bandwidth of 70 GHz is assumed in the simulation model, which results in a random modulation of the instantaneous pump power, and (ii) that the OPO signals grow from quantum noise in the simulations. Figure 2(a) indicates that a crystal length of 8 mm would be optimal in terms of conversion efficiency for a doubly resonant configuration, while a crystal length of 9 mm or more is optimal for a singly resonant configuration. However, Fig. 2(b) clearly shows that a singly resonant OPO gives better beam quality than a doubly resonant configuration because back-conversion is minimized in a singly resonant design. The build-up time of the OPO needs to be short to obtain output pulses with similar duration as the pump pulses, to achieve high conversion in the OPA stage. Figure 2(c) plots the relative delay between the OPO output and the pump pulses as function of crystal length, and we observe that this delay is minimised by choosing a crystal length of 8 mm or more. As shown in Fig. 2(d), the simulated peak fluence is below 0.8 J/cm^2 for the singly resonant configuration, which is well below the damage threshold of the nonlinear crystal and the mirror coatings.

Based on the simulations, we chose a singly resonant configuration, where all resonator mirrors were HT for the idler ($T > 95\%$ at 4.3–4.9 μm). The signal out-coupling was 0.5. In

#207849 - $15.00 USD Received 7 Mar 2014; accepted 25 Mar 2014; published 2 Apr 2014

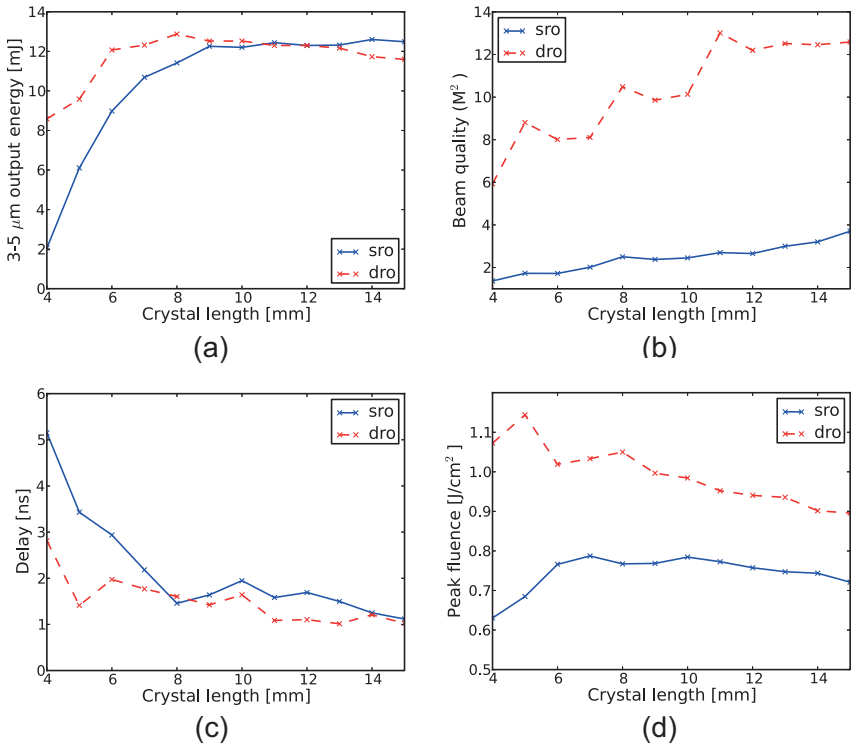

Fig. 2. Simulation results for the master oscillator with a pump pulse energy of 25 mJ. (a) output energy, (b) beam quality, (c) relative delay between OPO output and pump, and (d) internal peak fluence in the OPO cavity as a function of ZGP length. sro: singly resonant OPO, dro: doubly resonant OPO.

addition, the out-coupler was HR for the pump to allow for two-pass pumping. The remaining two OPO mirrors were HT for the pump and HR for the signal. The OPO performance was tested with one or two 6 mm long ZGP crystals, giving a total ZGP length of 6 mm or 12 mm in the OPO resonator. The ZGP length chosen for the OPO in the experiments reported below was 12 mm, because this length gave good conversion efficiency and short build-up time, resulting in output pulses with similar duration as the pump pulses. According to the simulations, a crystal length of ~ 9 mm would be slightly better in terms of beam quality, without sacrificing conversion efficiency, but this crystal length was not available during the experiments.

2.2. *Power amplifier*

The power amplifier was tested with 1–3 ZGP crystals, each 6 mm long, giving a total ZGP length of 6, 12, or 18 mm, to find the optimal crystal length. Walk-off compensation was not necessary due to the large diameters of the beams. The pump pulses were delayed 1 ns, compared to the seed pulses, to compensate for the build-up time of the OPO.

Figure 3 shows a selection of the simulation results for the power amplifier, where the output from the OPO simulation (singly resonant configuration with 12 mm ZGP length in the OPO cavity) was used to seed the OPA. The pump energy was 380 mJ, the pump diameter (FWe^{-2}M) 8.6 mm, the seed diameter (FWe^{-2}M) 8.7 mm, and the pump delay with respect to the seed 1 ns in the simulations. We observe from Fig. 3(a) that using both the signal and idler from the

#207849 - $15.00 USD Received 7 Mar 2014; accepted 25 Mar 2014; published 2 Apr 2014

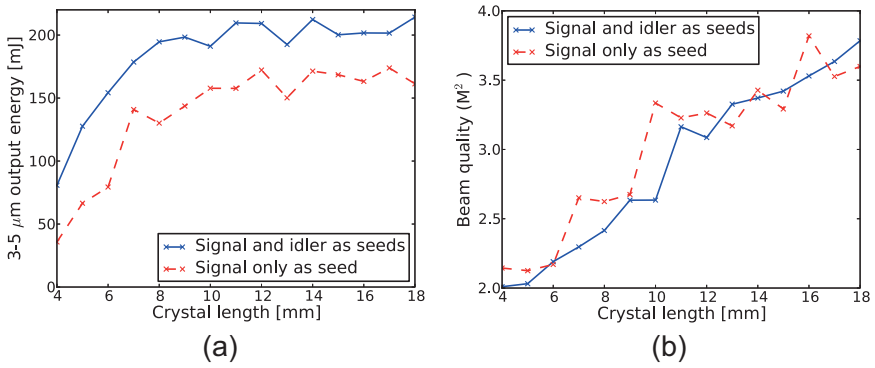

Fig. 3. Simulation results for the power amplifier with a pump pulse energy of 380 mJ. (a) output energy, and (b) beam quality. The OPA was simulated with the signal beam only from the master OPO as seed for the OPA, and with both the signal and idler beams as seed.

OPO to seed the OPA increases the output energy, compared to using the signal only as seed. This was also confirmed in the experiments. Also, the beam quality is not affected by using both the signal and idler as seed, as shown in Fig. 3(b). A crystal length of about 12 mm in the OPA is optimal because this maximizes the output energy, while maintaining a reasonably good beam quality. Increasing the ZGP length further results in worse beam quality, due to back-conversion, without increasing the output energy.

In a previous setup we have observed that the coatings on the front and back surface of the OPA crystals may act as resonator mirrors for a type I, non-collinearly phase-matched parasitic OPO process [5]. Parasitic signals at 2.5–3 μm and at 5.5 μm are phase-matched for the crystal cut angle of $\theta = 54^\circ$ used here. The crystal coatings were specified to have less than 10% reflection at these wavelengths to avoid problems with parasitic oscillation, in addition to being AR at the pump, signal, and idler wavelengths.

3. Experimental results

3.1. Master oscillator

Figure 4 shows the measured output energy (signal and idler) from the OPO. The threshold is 4.2 mJ, and the slope efficiency is 0.56. During operation of the MOPA, we used a pump energy of 25 mJ, resulting in an OPO output energy of 12 mJ, which is in good agreement with the simulations. The inset in Fig. 4 shows the measured far field fluence (signal and idler) from the OPO at 25 mJ pump energy. The corresponding beam quality of the OPO is $M^2 = 2.7$, based on measured second moments of the near- and far field. The output spectrum from the OPO is shown in Fig. 5, which is in reasonable agreement with the calculated parametric gain bandwidth of the nonlinear crystals in the OPO.

3.2. Power amplifier

Figure 6 shows the measured output energy (signal and idler) from the OPA for different number of ZGP crystals. For the maximum pump energy of 380 mJ, we obtained 136 mJ, 207 mJ, and 212 mJ, respectively, with 1–3 ZGP crystals. The measured output energy agrees well with the simulations for two and three ZGP crystals in the OPA, but the simulations overestimate the pulse energy for one ZGP crystal. No parasitic processes were observed at full pump and seed

#207849 - $15.00 USD Received 7 Mar 2014; accepted 25 Mar 2014; published 2 Apr 2014

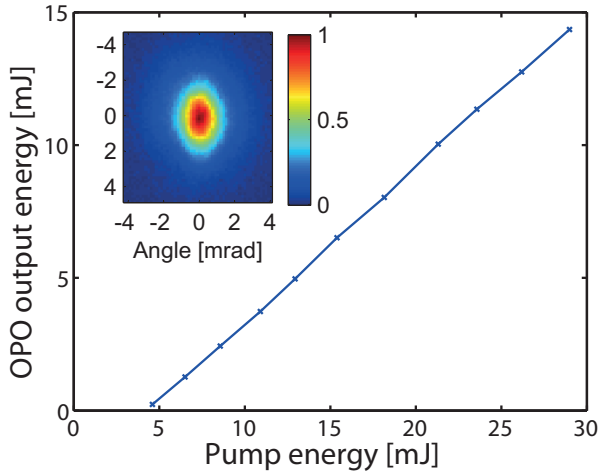

Fig. 4. Measured OPO output energy (signal and idler). The inset shows measured far field fluence from the OPO at 25 mJ pump energy.

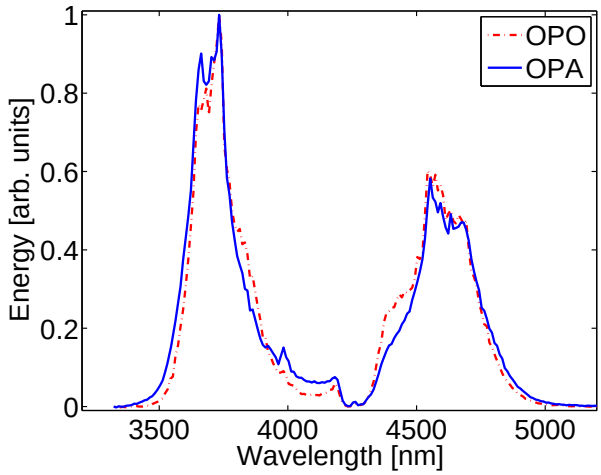

Fig. 5. Measured output spectrum (signal and idler) from the OPO and the OPA.

power.

Figure 7 shows the measured near- and far field fluence distributions from the OPA (signal and idler) at full pump energy, with three ZGP crystals in the OPA. The near field of the OPA output resembles the fluence profile of the pump beam in the position of the OPA, while the far field resembles the far field of the OPO. Based on the second moments of the near- and far field of the OPA output (signal and idler) at maximum pump energy, we obtain a beam quality of M^2 =2.7, 2.9, and 3.3, respectively, for 1–3 ZGP crystals. Backconversion is the probable cause of the measured degradation of beam quality with increasing crystal length.

The measured spectrum of the OPA is shown in Fig. 5. We observe that the OPA spectrum is similar to the OPO spectrum. The dip in the measured spectra at 4.2–4.3 μm is due to absorption by CO_2 in air.

#207849 - $15.00 USD
(C) 2014 OSA
Received 7 Mar 2014; accepted 25 Mar 2014; published 2 Apr 2014
7 April 2014 | Vol. 22, No. 7 | DOI:10.1364/OE.22.008556 | OPTICS EXPRESS 8562

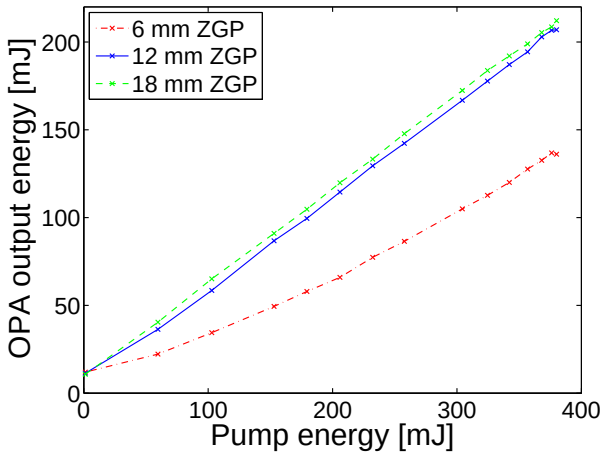

Fig. 6. Measured OPA output energy (signal and idler) for different number of ZGP crystals (1–3) in the OPA. The seed energy was 12 mJ.

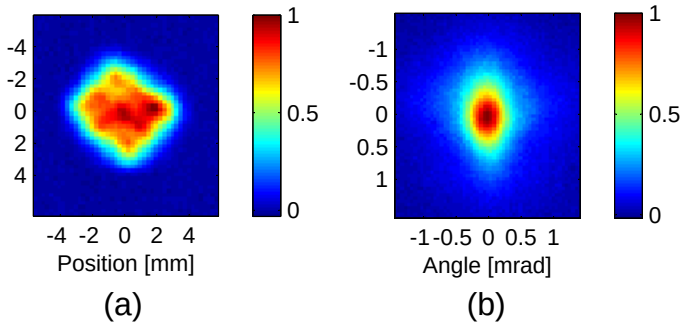

Fig. 7. Measured near field (a) and far field (b) fluence profiles from the OPA (signal and idler) at full pump energy, with 3 ZGP crystals in the OPA.

4. Discussion

The present MOPA shows good conversion efficiency and reasonably good beam quality. According to the simulations shown in Fig. 2, a beam quality of M^2 =1.5–2 could be achieved from the OPO by using a shorter ZGP length, at the expense of increased build-up time and lower pulse energy. Such pulses would be less suitable for seeding the OPA. The relation between build-up time and beam quality of the OPO is a general effect caused by cumulative spatial filtering by multiple passes through the OPO cavity during build-up [27]. There is thus a tradeoff between pulse energy and beam quality of the OPO. It is well known that lateral walk-off between the signal and idler restricts the phase-matching acceptance angle, thus improving the beam-quality in the walk-off direction. Lateral walk-off between the signal and idler is negligible in collinear type I parametric interactions, but can be large in non-collinear type I parametric processes. Smith and Bowers have suggested that noncollinear interactions in a type I phase-matched process can be used to improve the beam quality of OPOs with image-rotating cavities [16]. Using such an OPO geometry could improve the beam quality of the seed OPO while obtaining high pulse energy [17].

#207849 - $15.00 USD Received 7 Mar 2014; accepted 25 Mar 2014; published 2 Apr 2014

5. Conclusion

In summary, we have demonstrated a ZGP MOPA based on a singly resonant V-shaped 3-mirror ring OPO and an OPA with large-aperture ZGP crystals. 15 ns long pulses with more than 200 mJ energy in the 3–5 μm wavelength range are obtained, with beam quality $M^2 = 3$. To our knowledge, this is the highest pulse energy generated in this wavelength region by a nanosecond solid-state laser source.

#207849 - $15.00 USD Received 7 Mar 2014; accepted 25 Mar 2014; published 2 Apr 2014